CHEMISTRY OF MATERIALS

ARTICLE

pubs.acs.org/cm

Synthesis of Metallic Nanoparticles Using Electrogenerated Reduced Forms of $[\alpha\text{-}SiW_{12}O_{40}]^{4-}$ as Both Reductants and Stabilizing Agents

Jie Zhang, Boon Ping Ting, Yan Tong Koh, and Jackie Y. Ying*

Institute of Bioengineering and Nanotechnology, 31 Biopolis Way, The Nanos, Singapore 138669

Supporting Information

ABSTRACT: In this paper, controlled potential bulk electrolysis at a glassy carbon working electrode was conveniently employed to produce the reduced forms of $H_4[\alpha\text{-}SiW_{12}O_{40}]$ with little or no supporting electrolyte. Consequently, without the need for separation and purification, these reduced forms of $[\alpha\text{-}SiW_{12}O_{40}]^{4-}$ were directly used as both the reductants and the stabilizing agents for the size-controlled synthesis of various types of metallic and alloy nanoparticles, including Au, Ag, Pt, Pd and Ag−Au. Ni nanoparticles were also successfully synthesized using highly reduced $[\alpha\text{-}SiW_{12}O_{40}]^{4-}$ under neutral pH condition. The Pt nanoparticles thus obtained displayed attractive electrocatalytic properties in methanol oxidation.

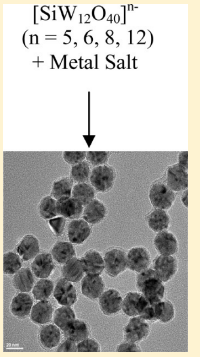

KEYWORDS: metallic nanoparticles, electrolysis, polyoxometalate, $[\alpha\text{-}SiW_{12}O_{40}]^{4-}$, reductant, stabilizing agent

INTRODUCTION

There has been an increasing interest in metal and semiconductor nanocrystals over the past decade, as a result of their quantum confinement effects and unique electronic, optical, and catalytic properties.[1−6] Because these properties are extremely sensitive to the size, shape, and composition of the nanocrystals, novel materials can be derived via the careful control of crystallite size, morphology, and composition.[1−6]

Polyoxometalates (POMs) are stable and highly negatively charged cluster anions that exhibit a wide range of structural, redox, and catalytic properties (see Scheme 1).[7−11] POMs can be adsorbed onto the surface of nanocrystals to produce strongly repulsive electrostatic forces, hence stabilizing the nanocrystals against aggregation.[12−14] Therefore, their initial role in nanoparticle synthesis is to act solely as a stabilizing reagent.[12,13]

Because POMs also exhibit rich redox properties, in principle, they can serve as reductants to reduce metallic ions to zero valence metals. Consequently, metallic nanoparticles can be synthesized with POMs acting as both the reducing and the stabilizing agents.[15−25] A key step in this synthesis is to generate the reduced form of the POMs. This can be achieved by (1) photolysis, where the excited-state POMs are reduced by a wide variety of organic substances,[15,16] (2) electrolysis,[17] (3) radiolysis in the presence of 2-propanol,[18] and (4) chemical synthesis that directly has the reducing capability.[19]

The concept of using POMs as both the reducing and the stabilizing reagents was first developed by Papaconstantinou and co-workers who synthesized metal nanocrystals in aqueous media using reduced Keggin POMs generated from a photocatalytic redox reaction with 2-propanol.[20] This approach was used subsequently by Sastry and co-workers to synthesize Au@Ag core−shell nanocrystals in aqueous medium.[21] The key steps involved in the synthesis are summarized in eqs 1−4:

$$2POM^{n-} + (CH_3)_2CHOH \xrightarrow{h\nu} 2POM^{(n+1)-} + (CH_3)_2C{=}O + 2H^+ \quad (1)$$

$$POM^{(n+1)-} + M^+ \rightarrow POM^{n-} + M \quad (2)$$

$$xM \xrightarrow{\text{nucleation/growth}} \text{unstable nanocrystal} \quad (3)$$

$$\text{unstable nanocrystal} \xrightarrow{\text{adsorption of } POM^{n-}} \text{stable nanocrystal} \quad (4)$$

where M^+ and M are metal cation and metal atom, respectively.

More recently, chemical methods have also been used to synthesize the reduced forms of POMs for the same purposes.[22−25] In these papers, Nadjo and co-workers reported their efforts in the chemical synthesis of a wide range of reduced forms of POMs with different reversible potentials, which could be further used in the synthesis of Pd, Pt, Au, and Ag nanoparticles and Ag nanowires. These studies have been summarized in a review article.[19]

Bulk electrolysis has been proven to be a very effective method for the synthesis of chemical reagents in different redox states,[26,27] since (i) it is efficient, typically taking ~30 min for complete bulk electrolysis, and (ii) the electrode can serve as the reducing agent. Therefore, the introduction of additional reducing agents can be avoided. However, despite having these attractive features, the

Received: April 24, 2011
Revised: September 8, 2011
Published: October 04, 2011

Scheme 1. Structure of Keggin POM $[\alpha\text{-SiW}_{12}O_{40}]^{4-}$ Used in This Study[a]

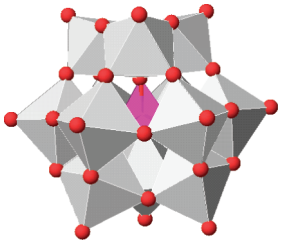

[a] The red spots represent oxygen atoms, the purple center represents Si, and the metal center is located within every polyhedral structure (not visible in this representation).

bulk electrolysis method has not been used in the synthesis of reduced forms of POMs for the direct derivation of nanoparticles. This is presumably due to the fact that the supporting electrolyte traditionally employed in the bulk electrolysis is expected to destabilize the electrostatically stabilized nanoparticles. Therefore, the removal of the supporting electrolyte is required prior to the nanoparticle synthesis. However, in principle, the supporting electrolyte may not be required for the bulk electrolysis of POM in aqueous medium because POM itself would be mostly dissociated in this high dielectric constant medium to provide sufficiently high ionic conductivity. Consequently, the reduced form of POM generated in this way did not require further separation and purification prior to its use in nanoparticle synthesis. Equation 5 summarizes the simple electrochemical reaction in place of the photochemical and chemical processes of eq 1.

$$POM^{n-} + e^- \xrightarrow{\text{electrode}} POM^{(n+1)-} \quad (5)$$

POMs contain multiple metal centers. Each metal center, in principle, can undergo at least one single-electron transfer reaction.[28] Therefore, POMs have the ability to accept multiple electrons (e.g., in principle, $[\alpha\text{-SiW}_{12}O_{40}]^{4-}$ can accept up to 12 electrons) without decomposition. Using the electrochemical method, it is possible to generate multiple electron-reduced forms by simply applying a more negative potential. These multiple electron-reduced forms are more powerful reductants, as compared to their one electron-reduced counterpart. Although bulk electrolysis has been used in the conventional way to synthesize the reduced forms of POMs in the presence of excessive amount of supporting electrolyte,[29,30] the POMs generated in this way have not been applied toward nanoparticle synthesis.

In this paper, controlled potential bulk electrolysis was employed to produce the reduced forms of $[\alpha\text{-SiW}_{12}O_{40}]^{4-}$ with little or no supporting electrolyte. The reduced forms of $[\alpha\text{-SiW}_{12}O_{40}]^{4-}$ were used as both the reductants and the stabilizing agents for synthesizing various types of metallic and alloy nanoparticles. The Pt nanoparticles thus obtained were employed as effective electrocatalysts for methanol oxidation.

EXPERIMENTAL SECTION

The $H_4[\alpha\text{-SiW}_{12}O_{40}]$, $HAuCl_4$, Na_2PdCl_4, K_2PtCl_4, H_2PtCl_6, $AgNO_3$, $Ni(CH_3COO)_2$, H_2SO_4, methanol, and 5% Nafion 117 solution were purchased from Sigma Aldrich. The carbon black supported Pt nanoparticle catalyst was purchased from Johnson Matthey.

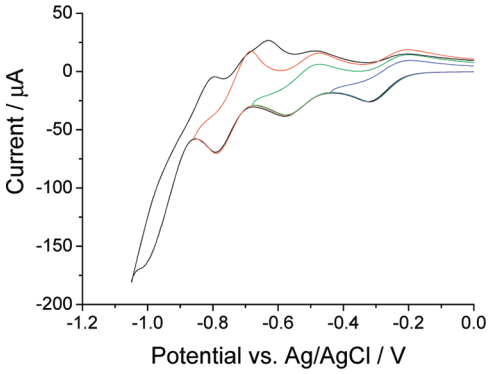

Figure 1. Cyclic voltammograms obtained with different switching potentials of −1.05 V (black), −0.86 V (red), −0.68 V (green), and −0.44 V (blue), at a scan rate of 0.1 V/sec, for the reduction of 2.0 mM of $[\alpha\text{-SiW}_{12}O_{40}]^{4-}$ at a 3 mm diameter glassy carbon electrode.

$H_4[\alpha\text{-SiW}_{12}O_{40}]$ (2−5 mM) underwent bulk electrolysis using a three-electrode electrochemical cell, with a glassy carbon beaker as the working electrode, Ag/AgCl (3 M KCl) as the reference electrode, and Pt gauze as the counter electrode. A CHI 760C potentiostat (CH Instruments, Inc., Texas, U.S.A.) was used for controlled potential electrolysis. The $H_4[\alpha\text{-SiW}_{12}O_{40}]$ solution was purged with N_2 gas to remove O_2 and to increase the mass transport rate during the electrolysis (~20−40 min). The reduced forms of $[\alpha\text{-SiW}_{12}O_{40}]^{4-}$ were added to millimolar or submillimolar levels of metal ions or mixtures of different metal ions to produce the respective nanoparticles. A sufficient amount of the reduced forms of $[\alpha\text{-SiW}_{12}O_{40}]^{4-}$ was used in all studies to ensure that all metal ions could be reduced to metal, on the basis of the stoichiometry of the redox reactions. All experiments were conducted at 25 °C. Transmission electron microscopy (TEM) experiments were performed on a JEOL JEM-3010 electron microscope (200 kV).

For the preparation of a Pt-modified electrode, a known amount of Pt nanoparticles was dissolved in 0.2 mL of diluted Nafion solution (5% Nafion in low aliphatic alcohols, diluted 10 times in deionized water) and 1 mL of deionized water. Lastly, 5 μL of the solution was transferred to a 2 mm diameter glassy carbon electrode using a micropipet. This electrode was left to dry in air, which resulted in a glassy carbon electrode modified with a thin film of Pt nanoparticle catalyst. The typical loading of Pt was 14 $\mu g\ cm^{-2}$.

RESULTS AND DISCUSSION

Electrochemistry of $[\alpha\text{-SiW}_{12}O_{40}]^{4-}$ in the Aqueous Phase in the Absence of Added Supporting Electrolyte and the Stability of Its Reduced Forms. Although the electrochemistry of POMs is well-documented,[28,31] voltammetric studies of POMs in the absence of added supporting electrolyte are rare. Bond and co-workers[32] have reported the cyclic voltammetric studies on $[SMo_{12}O_{40}]^{2-}$ and $[SMo_{12}O_{40}]^{3-}$ and the reversible reduction of $[S_2Mo_{18}O_{62}]^{4-}$ to $[S_2Mo_{18}O_{62}]^{5-}$ and $[S_2Mo_{18}O_{62}]^{6-}$, at a macrodisk electrode in acetonitrile,[33] in the absence of added supporting electrolyte.

Herein, cyclic voltammetric studies were first conducted to investigate the electrochemical properties of $[\alpha\text{-SiW}_{12}O_{40}]^{4-}$ in the absence of supporting electrolyte. Figure 1 shows a total of four well-defined voltammetric processes within the potential window with midpotentials (average of anodic and cathodic peak potentials) of −0.258 V, −0.524 V, −0.736 V, and −0.914 V versus a Ag/AgCl (3 M KCl) reference electrode. The first two

dx.doi.org/10.1021/cm201166t |Chem. Mater. 2011, 23, 4688–4693

processes were one-electron reduction processes and were relatively pH-insensitive. The third process was a proton-coupled two-electron process under these conditions, and its reversible potential was highly pH-sensitive, because a highly negatively charged reduced polyanion is a stronger base.[34] The fourth process was a four-electron process with protons coupled to the electron transfer. This process had much more complex voltammetric features than the third process, because the kinetics of proton transfer played a role in determining the characteristics of the voltammogram in the time scale of the measurements.[35,36] Its reversible potential was even more pH-sensitive than the third process, because the species involved in this process have a larger number of negative charges and, hence, were stronger bases.

Moreover, because the supporting electrolyte was absent, the contribution of migration to mass transport and the electric double layer effect also influenced the shape of the voltammogram. A full interpretation of the voltammetric results would require further theoretical studies and was beyond the scope of this paper. However, it was important to confirm the stability of the reduced forms and the chemical reversibility between the reduced forms and the starting material. Thus, the solutions containing the reduced forms of $[\alpha\text{-}SiW_{12}O_{40}]^{4-}$ were purged with O_2 after electrolysis to reoxidize them to their original form, $[\alpha\text{-}SiW_{12}O_{40}]^{4-}$. As expected in all cases, the blue solutions of the reduced forms turned colorless, as seen in the $[\alpha\text{-}SiW_{12}O_{40}]^{4-}$ solution. Quantitative measurements of the peak current after voltammetric measurements on these colorless solutions confirmed that the decomposition of $[\alpha\text{-}SiW_{12}O_{40}]^{n-}$ ($n \geq 4$) was insignificant for all the processes of interest in the time scale involved (typically <1 h). The redox ability of a species was indicated by its reversible potential. The more negative the reversible potential, the more powerful reductant was the reduced form. Therefore, the redox ability of the third and fourth reduced forms of $[\alpha\text{-}SiW_{12}O_{40}]^{4-}$ could be varied significantly by changing the pH of the reaction medium, which would be an additional advantage of using these two reduced forms for nanoparticle synthesis.

Synthesis of Metallic Nanoparticles Using $[SiW_{12}O_{40}]^{5-}$. The bulk electrolysis of $[\alpha\text{-}SiW_{12}O_{40}]^{4-}$ was first performed at a potential of −0.4 V to generate $[SiW_{12}O_{40}]^{5-}$. Subsequently, the reduced form was added to the following metal ion solutions, $AuCl_4^-$, $PtCl_4^{2-}$, $PdCl_4^{2-}$, and Ag^+. The amount of $[SiW_{12}O_{40}]^{5-}$ was chosen on the basis of the stoichiometry of the redox reactions. The solution was purged with N_2 to remove O_2 and to mix the reactants uniformly. Because the reactions were thermodynamically favorable,[20] the solutions turned pink for Au nanoparticles, brownish black for Pt and Pd nanoparticles, and yellow for Ag nanoparticles after several seconds (UV−vis spectra of Au and Ag nanoparticles are shown in Figure S1 in the Supporting Information). TEM studies confirmed the formation of nanoparticles with diameters of 15 ± 3, 4.5 ± 0.5, 8 ± 1, and 17 ± 3 nm for Au, Pt, Pd, and Ag, respectively (Figure 2). These nanoparticles are stable in solution for at least one week. These results were consistent with the findings of Troupis and coworkers when photochemically generated $[SiW_{12}O_{40}]^{5-}$ was used.[20] The composition of POM-stabilized metallic nanoparticles has been characterized previously by Lin and Finke, who suggested the adsorption of POM anion rather than its countercation to the nanoparticle surface, on the basis of the results of the surface charge measurement.[37]

Inductively coupled plasma mass spectroscopy (ICP-MS) also confirmed the presence of $[\alpha\text{-}SiW_{12}O_{40}]^{4-}$. Because the size of

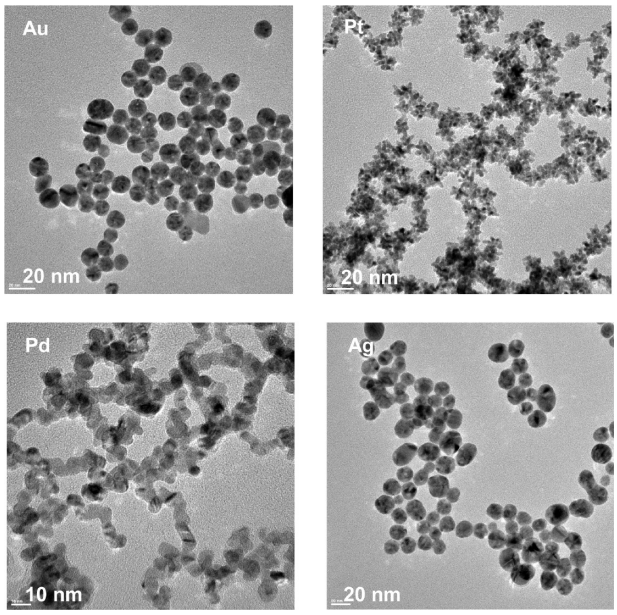

Figure 2. Nanoparticles synthesized with $[SiW_{12}O_{40}]^{5-}$.

$[\alpha\text{-}SiW_{12}O_{40}]^{4-}$ was known to be ~1 nm,[2,8] and because the nanoparticle size was also known, the maximum number of $[\alpha\text{-}SiW_{12}O_{40}]^{4-}$ on the nanoparticle surface could be estimated. Our analysis suggested that not all of the $[\alpha\text{-}SiW_{12}O_{40}]^{4-}$ species were adsorbed on the nanoparticle surface. In fact, most of the $[\alpha\text{-}SiW_{12}O_{40}]^{4-}$ species were not in direct contact with the nanoparticle surface, as indicated also by the high-resolution TEM images. Some of the $[\alpha\text{-}SiW_{12}O_{40}]^{4-}$ species might exist as counterions in the solution, as suggested previously.[37]

We have also examined the effect of higher $[SiW_{12}O_{40}]^{5-}$ to $AuCl_4^-$ ratios (up to 2.5 times the stoichiometric ratio) on the size and morphology of the Au nanoparticles. The results showed that the size and morphology of the Au nanoparticles remained largely the same.

Effect of Different Reduced Forms of $[\alpha\text{-}SiW_{12}O_{40}]^{4-}$ on the Morphologies of the Metallic Nanoparticles. To have a fair comparison, the ratios of the reduced forms of $[\alpha\text{-}SiW_{12}O_{40}]^{4-}$ to the metal ions used in these experiments were chosen on the basis of the stoichiometry of the redox reactions when $[SiW_{12}O_{40}]^{5-}$ was used as the reductant, and they were kept unchanged for the other reduced forms. The Pt nanoparticles have a "flower" morphology. The number of "petals" decreased when $[SiW_{12}O_{40}]^{6-}$, $[SiW_{12}O_{40}]^{8-}$, and $[SiW_{12}O_{40}]^{12-}$ were used instead of $[SiW_{12}O_{40}]^{5-}$ (Figure 3). The diameter of each petal also decreased from 4.5 ± 0.5 nm for the case of $[SiW_{12}O_{40}]^{5-}$ to 3.5 ± 0.4 nm for the other cases (Table 1). This decrease in nanoparticle diameter was also observed in the cases of Au (~15 ± 3 nm for $[SiW_{12}O_{40}]^{5-}$ and ~8 ± 1 nm for the other reduced forms of $[\alpha\text{-}SiW_{12}O_{40}]^{4-}$) and Pd (~8 ± 1 nm for $[SiW_{12}O_{40}]^{5-}$ and ~5.5 ± 0.5 nm for the other reduced forms of $[\alpha\text{-}SiW_{12}O_{40}]^{4-}$). However, in the case of Ag, the size remained almost unchanged when different reduced forms were used. Formation of smaller Pt, Au, and Pd nanoparticles in the presence of stronger and more negatively charged POMs could be expected. This was because when a stronger reductant was used, the reduction of ions occurred at a faster rate, which resulted in the production of smaller nanoparticle nuclei as a result of more rapid nucleation. This was also observed

dx.doi.org/10.1021/cm201166t |Chem. Mater. 2011, 23, 4688–4693

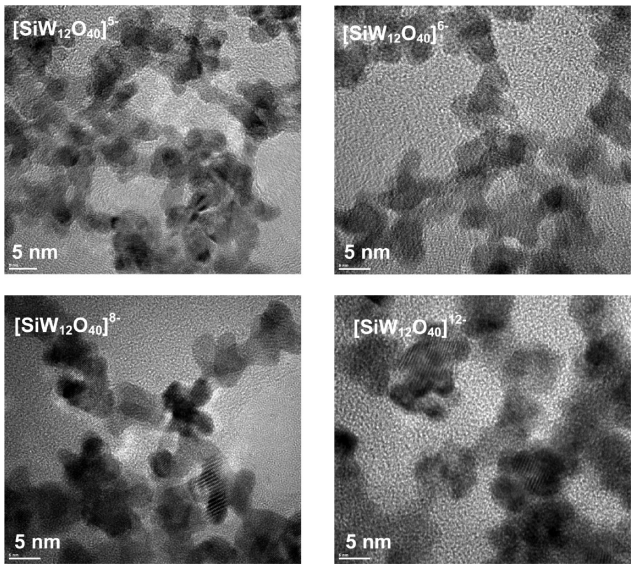

Figure 3. Pt nanoparticles synthesized with the different reduced forms of $[\alpha\text{-}SiW_{12}O_{40}]^{4-}$.

previously by the other researchers.[38−41] Moreover, the stronger reductants contained more negative charges in our case. Therefore, they were expected to be stronger stabilizing reagents that favored the formation of smaller nanoparticles. Even though the more negatively charged POMs were stronger reductants, the situation might be more complicated in the case of Ag because the more negatively charged POMs could form complexes with positively charged Ag^+ and this might slow down the reduction rate of Ag^+. Metallic nanoparticles synthesized through the use of POMs have been documented, but the photochemically reduced form of POMs was mostly the first reduced form.[20,21] This work showed that size control of the nanoparticles could be achieved using the different reduced forms conveniently derived by reducing the POMs electrochemically.

Effect of Supporting Electrolyte on the Formation and the Stability of the Metallic Nanoparticles. In electrochemistry, excess supporting electrolyte (typically 100 times the analyte concentration) is often used to increase the solution's ionic conductivity and to simplify theoretical analysis.[27] However, the presence of an electrolyte could affect the nanoparticle formation. The stabilization of nanoparticles by polyanions was based on electrostatic repulsion,[42] which would be weakened in the presence of supporting electrolyte according to the Gouy−Chapman theory.[27] Therefore, experiments were also conducted to investigate the effect of an acidic supporting electrolyte (e.g., H_2SO_4) on the formation of nanoparticles. Acid was chosen in this study because it could be used to increase the solubility of K^+ or Na^+ salts of POMs in water. The results suggested that all the nanoparticles mentioned above could be synthesized in the presence of millimolar levels of H_2SO_4. In most cases, the presence of millimolar levels of H_2SO_4 did not have a significant effect on the size and morphology of the nanoparticles. However, in the case of Ag, the presence of millimolar levels of H_2SO_4 increased the nanoparticle diameter from 17 to 45 nm when $[SiW_{12}O_{40}]^{5-}$ was used as the reductant. Higher concentrations of H_2SO_4 would destabilize the Ag nanoparticles and cause irreversible aggregation.[43] Therefore, bulk electrolysis in the presence of low supporting electrolyte concentration, if required, could be used to produce reduced POMs for nanoparticle synthesis without the need for separation and purification of the reduced POMs.

Table 1. Voltammetric Results of Methanol Oxidation at Glassy Carbon Electrodes Modified with Different Pt Nanoparticles[a]

POM reductant	Pt nanoparticle dia. (nm)	peak current density[b] (mA cm^{-2})	anodic potential vs Hg/Hg_2SO_4 (V)
$[SiW_{12}O_{40}]^{5-}$	4.5	0.95 ± 0.09	0.171 ± 0.008
$[SiW_{12}O_{40}]^{6-}$	3.5	1.00 ± 0.10	0.167 ± 0.006
$[SiW_{12}O_{40}]^{8-}$	3.5	0.97 ± 0.10	0.172 ± 0.008
$[SiW_{12}O_{40}]^{12-}$	3.5	1.02 ± 0.12	0.170 ± 0.007

[a] Experimental conditions were the same as those mentioned in the caption of Figure 5. [b] Surface area of Pt nanoparticles was estimated on the basis of the protocol described in the Supporting Information.

Synthesis of Ni Nanoparticles. The synthesis of Ni nanoparticles was of special interest because of their magnetic properties. Our results suggested that $[SiW_{12}O_{40}]^{5-}$, $[SiW_{12}O_{40}]^{6-}$, and $[SiW_{12}O_{40}]^{8-}$ were unable to reduce Ni^{2+} to form Ni nanoparticles under various conditions and pH values. $[SiW_{12}O_{40}]^{12-}$ was also not powerful enough to reduce Ni^{2+} under acidic conditions, even though the reduction of Ni^{2+} to bulk Ni was −0.467 versus Ag/AgCl (3 M KCl), which was more positive than the reversible potentials of the second to fourth reduced forms of $[\alpha\text{-}SiW_{12}O_{40}]^{4-}$. This was most likely due to the fact that the initial reduction of Ni^{2+} to form a small cluster of a few atoms was expected to occur at a much more negative potential than the reduction of Ni^{2+} to form bulk Ni, as in the case of Ag^+ reduction.[44]

However, the addition of NaOH to the solution to adjust the pH to neutral condition generated a more powerful reductant for the Ni^{2+} reduction to form Ni nanoparticles. The Ni nanoparticles derived could be moved by a magnet. The TEM image in Figure 4 shows that the size of these nanoparticles was ∼20 nm. The formation of Ni nanoparticles using POM as both reductant and stabilizing agent has not been reported before, since the photochemically generated $[SiW_{12}O_{40}]^{5-}$ was not a sufficiently strong reductant. This further demonstrated the advantage of using the electrochemical method for the generation of the reduced forms of POMs for nanoparticle synthesis.

Synthesis of Ag−Au Alloy Nanoparticles. The application of POMs for the synthesis of binary alloy nanoparticles was also explored. The simultaneous reduction of a mixture of $AuCl_4^-$ and Ag^+ (molar ratio 5:4) by $[SiW_{12}O_{40}]^{5-}$, $[SiW_{12}O_{40}]^{6-}$, $[SiW_{12}O_{40}]^{8-}$, or $[SiW_{12}O_{40}]^{12-}$ produced alloy nanoparticles. The TEM image in Figure S2 in the Supporting Information shows that uniform nanoparticles were formed when $[SiW_{12}O_{40}]^{5-}$ was used. The UV−visible spectrum showed a peak shift from 400 nm for pure Ag nanoparticles and 520 nm for pure Au nanoparticles to 500 nm for the Au−Ag alloy nanoparticles. Energy dispersive X-ray (EDX) analysis also confirmed the presence of both Au and Ag. When $[SiW_{12}O_{40}]^{6-}$, $[SiW_{12}O_{40}]^{8-}$, or $[SiW_{12}O_{40}]^{12-}$ were used, smaller Au−Ag alloy nanoparticles were obtained.

Application of Pt Nanoparticles as Electrocatalyst for Methanol Oxidation. Pt nanoparticles are an effective anode catalyst for methanol oxidation. POM-stabilized Pt nanoparticles generated via chemical synthesis are efficient catalysts for alcohol oxidation.[23] The electrocatalytic properties of Pt nanoparticles synthesized in this study were examined for methanol oxidation. The Pt nanoparticle-modified electrode was prepared on the basis of a literature procedure.[45]

dx.doi.org/10.1021/cm201166t |*Chem. Mater.* 2011, 23, 4688–4693

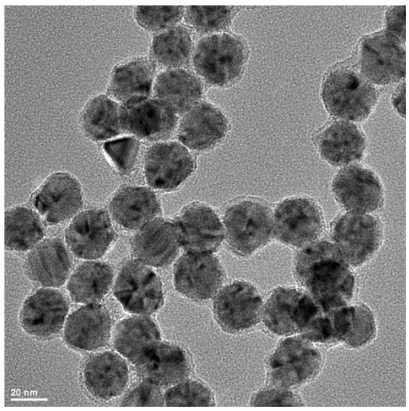

Figure 4. Ni nanoparticles synthesized under neutral pH with $[SiW_{12}O_{40}]^{12-}$ as the reductant and the stabilizing agent.

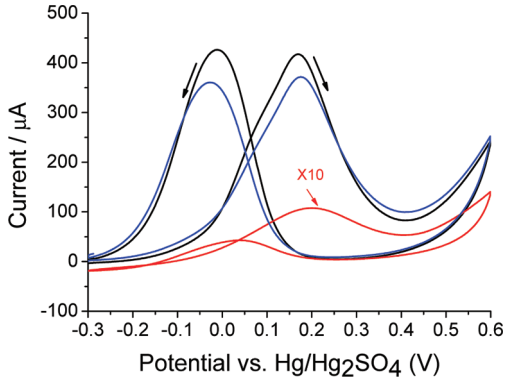

Figure 5. Cyclic voltammetric measurement in an aqueous solution containing 1 M methanol and 0.5 M H_2SO_4 at a 2 mm diameter rough Pt electrode (red) (current was multiplied by 10), commercial carbon black supported Pt nanoparticle modified electrode (blue), and Pt nanoparticle catalyst modified electrode (black). A scan rate of 50 mV s^{-1} was used.

The comparison was first made between the Pt nanoparticle catalyst synthesized using $[SiW_{12}O_{40}]^{12-}$ and the bulk Pt disk catalyst (Figure 5). To ensure a fair comparison, the surface areas of both catalysts were measured on the basis of the characteristic hydrogen adsorption process, obtained with a cyclic voltammetric measurement in a H_2SO_4 solution (0.5 M)[46,47] (see Figure S3 in the Supporting Information). The results showed that the Pt nanocatalyst had a surface area that was 7 times that of the Pt disk catalyst. The diameter of Pt nanoparticles was estimated to be ~3.3 nm on the basis of the surface area characterization, which was consistent with the TEM findings. The activity of the Pt catalysts toward methanol oxidation was determined by cyclic voltammetric measurements in an aqueous electrolyte solution containing 1 M methanol and 0.5 M H_2SO_4 (see Figure 5). In the forward potential scan, the adsorbed methanol was oxidized. In the reverse potential scan, the residual carbonaceous species generated from the forward potential sweep were oxidized to CO_2.[48] The peak current could provide information on the catalyst activity. The studies indicated that the Pt nanoparticles have a lower overpotential for methanol oxidation and were more than seven times more active than the bulk Pt disk, after the difference in their surface areas was taken into account. This result was qualitatively consistent with the results obtained by Nadjo and co-workers.[24]

In comparison with the commercial carbon black supported Pt nanoparticle catalyst, our Pt nanoparticle catalyst showed ~30% higher activity on the basis of the peak current, after the difference in their surface areas has been taken into account (see Figure S4 in the Supporting Information). The voltammetric results of methanol oxidation were also obtained with the Pt nanoparticle catalysts synthesized using the other three reduced forms of $[\alpha\text{-}SiW_{12}O_{40}]^{4-}$. The anodic potentials and the anodic peak current densities of the latter are presented in Table 1. The results indicated that both anodic potential and anodic peak current density were rather comparable in all cases. These results were consistent with those obtained by Nart and co-workers who suggested that the most active Pt nanoparticle catalysts for methanol oxidation were 3−10 nm in diameter, and the lower activity of either the smaller or larger Pt nanoparticles was mainly due to the partial oxidation of methanol to formaldehyde.[49]

CONCLUSIONS

In summary, the reduced forms of POMs could be easily generated electrochemically by controlled potential bulk electrolysis with little or no supporting electrolyte. The reduced forms of POMs were useful toward the synthesis of metallic and alloy nanoparticles with controlled size. The resulting Pt nanoparticles demonstrated attractive electrocatalytic properties toward methanol oxidation.

ASSOCIATED CONTENT

Supporting Information. UV−vis spectra of Au and Ag nanoparticles; TEM images of Au−Ag alloy nanoparticles; and measurement of Pt surface areas. This material is available free of charge via the Internet at http://pubs.acs.org.

AUTHOR INFORMATION

Corresponding Author
*E-mail: jyying@ibn.a-star.edu.sg.

ACKNOWLEDGMENT

This work was funded by the Institute of Bioengineering and Nanotechnology (Biomedical Research Council, Agency for Science, Technology and Research, Singapore).

REFERENCES

(1) Yin, Y.; Alivisatos, A. P. *Nature* **2005**, *437*, 664–670.
(2) Daniel, M. C.; Astruc, D. *Chem. Rev.* **2004**, *104*, 293–346.
(3) Murray, C. B.; Kagan, C. R.; Bawendi, M. G. *Annu. Rev. Mater. Sci.* **2000**, *30*, 545–610.
(4) (a) El-Sayed, M. A. *Acc. Chem. Res.* **2001**, *34*, 257–264. (b) Burda, C.; Chen, X. B.; Narayanan, R.; El-Sayed, M. A. *Chem. Rev.* **2005**, *105*, 1025–1102.
(5) (a) Yang, J.; Lee, J. Y.; Ying, J. Y. *Chem. Soc. Rev.* **2011**, *40*, 1672–1696. (b) Yang, J.; Sargent, E. H.; Kelley, S. O.; Ying, J. Y. *Nat. Mater.* **2009**, *8*, 683–689. (c) Yang, J.; Ying, J. Y. *Angew. Chem., Int. Ed.* **2011**, *50*, 4637–4643. (d) Selvan, S. T.; Patra, P. K.; Ang, C. Y.; Ying, J. Y. *Angew. Chem., Int. Ed.* **2007**, *46*, 2448–2452. (e) Jiang, J.; Gu, H.; Shao, H.; Devlin, E.; Papaefthymiou, G. C.; Ying, J. Y. *Adv. Mater.* **2008**, *20*, 4403–4407. (f) Xie, J.; Zheng, Y.; Ying, J. Y. *J. Am. Chem. Soc.* **2009**, *131*, 888–889.
(6) Roucoux, A.; Schulz, J.; Patin, H. *Chem. Rev.* **2002**, *102*, 3757–3778.
(7) Hill, C. L. *Chem. Rev.* **1998**, *98*, 1–2.

(8) Pope, M. T. *Heteropoly and Isopoly Oxometalates*; Springer-Verlag: Berlin, 1983.
(9) Pope, M. T.; Muller, A. *Angew. Chem., Int. Ed.* **1991**, *30*, 34–48.
(10) Zhang, J.; Bond, A. M.; MacFarlane, D. R.; Forsyth, S. A.; Pringle, J. M.; Mariotti, A. W. A.; Glowinski, A. F.; Wedd, A. G. *Inorg. Chem.* **2005**, *44*, 5123–5132.
(11) Long, D. L.; Burkholder, E.; Cronin, L. *Chem. Soc. Rev.* **2007**, *36*, 105–121.
(12) Finke, R. G. In *Metal Nanoparticles: Synthesis, Characterization and Applications*; Daniel, L. F., Colby, A. F., Eds.; Marcel Dekker: New York, 2002; pp 17−54.
(13) Aiken, J. D.; Finke, R. G. *Chem. Mater.* **1999**, *11*, 1035–1047.
(14) Lica, G. C.; Browne, K. P.; Tong, Y. Y. *J. Cluster Sci.* **2006**, *17*, 349–359.
(15) Papaconstantinou, E. *Chem. Soc. Rev.* **1989**, *18*, 1–31.
(16) Hiskia, A.; Mylonas, A.; Papaconstantinou, E. *Chem. Soc. Rev.* **2001**, *30*, 62–69.
(17) Vu, T.; Bond, A. M.; Hockless, D. C. R.; Moubaraki, B.; Murray, K. S.; Lazarev, G.; Wedd, A. G. *Inorg. Chem.* **2001**, *40*, 65–72.
(18) Papaconstantinou, E. *J. Chem. Soc. Faraday Trans.* **1982**, *78*, 2769–2772.
(19) Keita, B.; Liu, T.; Nadjo, L. *J. Mater. Chem.* **2009**, *19*, 19–33.
(20) Troupis, A.; Hiskia, A.; Papaconstantinou, E. *Angew. Chem., Int. Ed.* **2002**, *41*, 1911–1914.
(21) Mandal, S.; Selvakannan, P. R.; Pasricha, R.; Sastry, M. *J. Am. Chem. Soc.* **2003**, *125*, 8440–8441.
(22) Zhang, G.; Keita, B.; Dolbecq, A.; Mialane, P.; Secheresse, F.; Miserque, F.; Nadjo, L. *Chem. Mater.* **2007**, *19*, 5821–5823.
(23) Keita, B.; Mbomekalle, I. M.; Nadjo, L.; Haut, C. *Electrochem. Commun.* **2004**, *6*, 978–983.
(24) Keita, B.; Zhang, G.; Dolbecq, A.; Mialane, P.; Secheresse, F.; Miserque, F.; Nadjo, L. *J. Phys. Chem. C* **2007**, *111*, 8145–8148.
(25) Maayan, G.; Neumann, R. *Chem. Commun.* **2005**, 4595–4597.
(26) Kissinger, P.; Heineman, W. R. *Laboratory Techniques in Electroanalytical Chemistry*, 2nd ed.; Marcel Dekker: New York, 1996.
(27) Bard, A. J.; Faulkner, L. R. *Electrochemical Methods: Fundamentals and Applications*, 2nd ed.; John Wiley & Sons: New York, 2000.
(28) Bond, A. M. *Broadening Electrochemical Horizons: Principles and Illustration of Voltammetric and Related Techniques*; Oxford University Press: Oxford, 2003.
(29) Mialane, P.; Dolbecq, A.; Lisnard, L.; Mallard, A.; Marrot, J.; Secheresse, F. *Angew. Chem., Int. Ed.* **2002**, *41*, 2398–2401.
(30) Cooper, J. B.; Way, D. M.; Bond, A. M.; Wedd, A. G. *Inorg. Chem.* **1993**, *32*, 2416–2420.
(31) Keita, B.; Nadjo, L. In *Encyclopedia of Electrochemistry*; Bard, A. J., Stratmann, M., Eds.; Wiley-VCH: Weinheim, 2006; Vol. 7, pp 607−700.
(32) Bond, A. M.; Coomber, D. C.; Harika, R.; Hultgren, V. M.; Rooney, M. B.; Vu, T.; Wedd, A. G. *Electroanalysis* **2001**, *13*, 1475–1480.
(33) Bond, A. M.; Coomber, D. C.; Feldberg, S. W.; Oldham, K. B.; Vu, T. *Anal. Chem.* **2001**, *73*, 352–359.
(34) Zhang, J.; Goh, J. K.; Tan, W. T.; Bond, A. M. *Inorg. Chem.* **2006**, *45*, 3732–3740.
(35) Guo, S.-X.; Feldberg, S. W.; Bond, A. M.; Callahan, D. L.; Richardt, P. J. S.; Wedd, A. G. *J. Phys. Chem. B* **2005**, *109*, 20641–20651.
(36) Guo, S.-X.; Mariotti, A. W. A.; Schlipf, C.; Bond, A. M.; Wedd, A. G. *Inorg. Chem.* **2006**, *45*, 8563–8574.
(37) Lin, Y.; Finke, R. G. *J. Am. Chem. Soc.* **1994**, *116*, 8335–8353.
(38) Chen, Y.; Liew, K. Y.; Li, J. L. *Appl. Surf. Sci.* **2009**, *255*, 4039–4044.
(39) Gupta, V.; Scharff, P.; Miura, N. *Mater. Lett.* **2006**, *60*, 25–26.
(40) Panigrah, S.; Kundu, S.; Gosh, S. K.; Nath, S.; Pal, T. *J. Nanopart. Res.* **2004**, *6*, 411–414.
(41) Watzky, M. A.; Finney, E. E.; Finke, R. G. *J. Am. Chem. Soc.* **2008**, *130*, 11959–11969.
(42) Ott, L. S.; Finke, R. G. *Coord. Chem. Rev.* **2007**, *251*, 1075–1100.
(43) Troupis, A.; Hiskia, A.; Papaconstantinou, E. *New J. Chem.* **2001**, *25*, 361–363.
(44) Henglein, A. *Chem. Rev.* **1989**, *89*, 1861–1873.
(45) Schmidt, T. J.; Gasteiger, H. A.; Stab, G. D.; Urban, P. M.; Kolb, D. M.; Behm, R. J. *J. Electrochem. Soc.* **1998**, *145*, 2354–2358.
(46) Feltham, A. M.; Spiro, M. *Chem. Rev.* **1971**, *71*, 177–193.
(47) Biegler, T.; Rand, D. A. J.; Woods, R. *J. Electroanal. Chem.* **1971**, *29*, 269–277.
(48) Mancharan, R.; Goodenough, J. B. *J. Mater. Chem.* **1992**, *2*, 875–887.
(49) Bergamaski, K.; Pinheiro, A. L. N.; Teixeira-Neto, E.; Nart, F. C. *J. Phys. Chem. B* **2006**, *110*, 19271–19279.